Cement & Concrete Composites 34 (2012) 41–47

Contents lists available at ScienceDirect

Cement & Concrete Composites

journal homepage: www.elsevier.com/locate/cemconcomp

The role of residual cracks on alkali silica reactivity of recycled glass aggregates

Hamed Maraghechi [a], Seyed-Mohammad-Hadi Shafaatian [a], Gregor Fischer [b], Farshad Rajabipour [c,*]

[a] The Pennsylvania State University, 3127 Research Drive, State College, PA 16801, USA
[b] Technical University of Denmark, Building 118, 2800 Kgs., Lyngby, Denmark
[c] The Pennsylvania State University, 223B Sackett Building, University Park, PA 16802, USA

ARTICLE INFO

Article history:
Received 30 November 2010
Received in revised form 8 July 2011
Accepted 8 July 2011
Available online 23 July 2011

Keywords:
Recycled glass
Alkali-silica reaction
Crack
Annealing
Scanning electron microscope

ABSTRACT

Despite its environmental and economical advantages, crushed recycled glass has limited application as concrete aggregates due to its deleterious alkali-silica reaction. To offer feasible mitigation strategies, the mechanism of ASR should be well understood. Recent research showed that unlike some natural aggregates, soda-lime glass undergoes ASR within cracks in the interior of glass particles and not at glass–paste interface. These cracks originate during bottle crushing and propagate further by ASR. This paper examines whether glass aggregates could become innocuous if these cracks are healed by annealing or when the crack widths are smaller than a critical size. The results confirm that glass annealed at 650 °C for 40 min or particles containing cracks smaller than approximately 2.5 μm can be considered innocuous based on ASTM C1260. Also larger glass particles contain significantly higher percentages of reactive microcracks which may explain why ASR expansions are lowered by reducing the size of glass aggregates.

1. Introduction

The practice of recycling glass containers is growing in many countries. Unfortunately, a significant portion (~600,000 tons/year in the United States [1,2]) of the collected glass is not actually recycled into new glass; mainly due to the prohibitive shipping costs from collection points to remelting facilities. In addition, the majority of US domestic container glass production is in clear and amber colors; which makes recycling of the imported green containers challenging and costly. Similar problems have been reported in Europe, Australia, and the Middle East [3–7]. Large quantities of the post-consumer glass are currently land-filled or stockpiled in hopes that future technologies would allow a profitable use of this material [1].

Application of recycled glass in concrete as cement or aggregate replacement can be environmentally and sometimes economically advantageous as it converts large quantities of waste materials to value-added products and reduces the need for transportation by offering a local material resource [6]. In particular, the feasibility of using recycled glass as sand in concrete has been explored; and it was determined that concretes with desirable strength and workability can be produced by proper mixture proportioning and the use of water reducing admixtures [8]. The major technical obstacle, however, is the deleterious alkali-silica reaction (ASR). The amorphous silicate structure of glass dissolves in the alkaline pore solution of concrete and forms an alkali-silica gel which, in the presence of water, swells and cracks the concrete [9–11]. Previous research [5,6,12,13] has focused on relating the severity of ASR expansions to the size, content, and color of glass aggregates. In particular, it was found that expansions and cracking generally decrease by reducing the particle size of glass [5,6]. Fig. 1 provides an example in which mortars containing a combination of recycled glass sand and natural glacier sand were tested for ASR expansion according to ASTM C1260 [14]. Recycled glass made up 0–50% of the total sand on a weight basis. The results show that expansions tend to decrease by reducing the average size of glass particles. While a pessimum average size of 1.8 mm (associated with glass particles between #8 and #16 sieves) is observed, finer particles show significantly smaller expansions. This is counter-intuitive as ASR is considered to be a surface reaction and should accelerate by reducing the size of reactive aggregates.

The dependence of alkali-silica reactivity on particle size is not limited to glass aggregates. Previous works on natural reactive aggregates suggest that ASR expansions tend to increase by reducing the particle size, a trend opposite of that observed for recycled glass. In one of the earliest reports on size effect, Stanton [15] found that a siliceous magnesian limestone was more reactive with decreasing particle size from the range 2.0–5.6 mm to 0.6–2.0 mm, and ultimately 0.18–0.6 mm showing the highest expansions. Using the same aggregate, Vivian [16] observed a similar trend down to particles retained on #200 sieve (75 μm); but found that smaller particles (50–75 μm) only expanded after 6 months while even smaller particles (<50 μm) did not expand at all. Similar observations were made when testing opal aggregates which

* Corresponding author. Tel.: +1 814 863 0601; fax: +1 814 863 7304.
E-mail addresses: hym5061@psu.edu (H. Maraghechi), sxs1071@psu.edu (S. Shafaatian), gf@byg.dtu.dk (G. Fischer), farshad@psu.edu (F. Rajabipour).

0958-9465/$ - see front matter © 2011 Elsevier Ltd. All rights reserved.
doi:10.1016/j.cemconcomp.2011.07.004

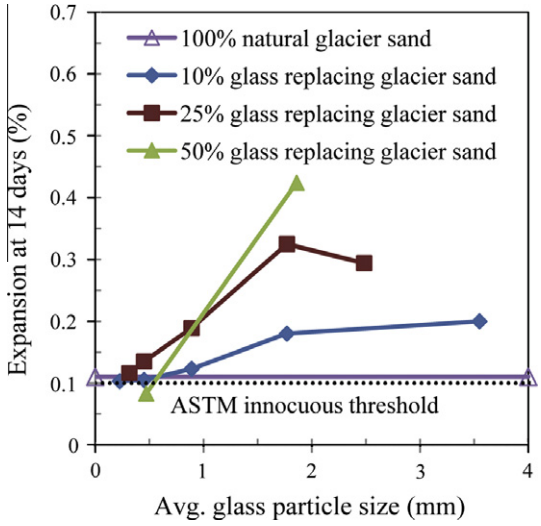

Fig. 1. Dependence of ASR expansion on the glass sand particle size in ASTM C1260 test (data from [14]).

resulted in maximum expansions in the range 50–75 μm particle size, with no expansion in particles smaller than 50 μm [16]. This reduced reactivity at extremely small particle sizes may be due to particles undergoing a pozzolanic reaction. Diamond and Thaulow [17] did not observe a monotonic relationship between expansion and particle size for opal sand, but noticed a general increase in expansion with smaller particles down to 20 μm. Hobbs and Gutteridge [18] reported a similar trend for a porous siliceous aggregate in the size range 0.15–4.72 mm.

To explain the origins of the unusual size-effect for recycled glass (which is the opposite of most natural reactive aggregates), a number of hypotheses have been offered. Bažant and Steffens [19] proposed a mathematical model for the kinetics of alkali-silica reaction as a combination of several diffusion-controlled mechanisms. This model suggests that the swelling pressure of the ASR gel strongly depends on the size of reactive aggregates and is maximum at some intermediate particle size. Further, Bažant et. al. [20] suggested a fracture mechanics-based explanation arguing that while the chemical reactions of ASR could accelerate by reducing the particle size (due to a larger surface area), the stress intensity factor is simultaneously and non-linearly reduced, favoring less cracking for smaller aggregates. As such, a pessimum particle size should exist resulting in the largest damage. Suwito et al. [21] hypothesized that smaller aggregates result in a larger volume of porous interfacial transition zone (ITZ) which provides space for free expansion of ASR gel without development of significant swelling stresses. It should be noted that these hypotheses are all based on the fundamental assumption that ASR occurs at the glass–cement paste interface. This assumption is intuitive, but was shown to be incorrect by SEM imaging for glass sand in mortar [3,22], as discussed in the next paragraph. In addition to these mechanisms, it has been argued that fine glass powder has pozzolanic properties [4,23,24] which can mitigate the ASR of larger particles. However, the pozzolanic reaction of glass was shown to be significant only for very fine particles (<38 μm) [25]. Such fine particles are absent in ASTM C1260 tests that resulted in the expansions shown in Fig. 1.

Our recent work [22] based on SEM imaging of mortar bars during ASTM C1260 test revealed that for soda-lime glass, ASR occurs within microcracks in the interior of glass particles and not at the glass–cement paste interface. Fig. 2a shows formation of ASR gel (confirmed by compositional EDS analysis) in the interior of a glass particle, while the glass–paste interface has seemingly remained

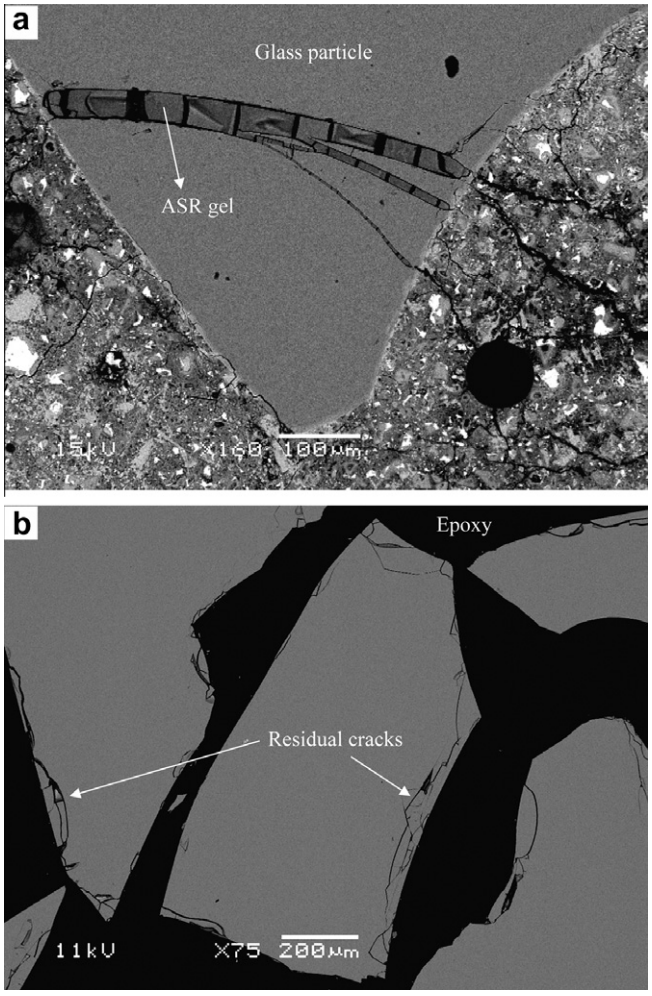

Fig. 2. (a) ASR affected glass particle (size range: 1.18–2.36 mm) showing intra-particle gel formation in mortar after 14 days in ASTM C1260 test and (b) Pre-existing microcracks in glass particles induced by bottle crushing.

intact. Several other SEM images of different magnifications are provided in [14,22]; all confirming the same observation. In addition, it was found that at least some of these microcracks originate during bottle crushing operations and are pre-existing before glass is used in concrete. Fig. 2b shows a SEM image of glass particles that were epoxy impregnated immediately after crushing. Despite no exposure to cement paste or alkalis, microcracks exist in glass particles. These microcracks are filled with epoxy, verifying that they were formed during bottle crushing and not during SEM sample preparation.

2. Research significance and objectives

As discussed, the recent work has led to the hypothesis that residual microcracks in the interior of crushed glass particles are responsible for occurrence of ASR and cracking in concrete. To better evaluate this hypothesis, this paper: (1) uses an annealing method to heal the residual microcracks and assess its impact on the reactivity of glass particles; and (2) uses an SEM image analysis procedure to determine if there is a critical crack size below which microcracks do not vigorously participate in ASR and to examine if smaller glass particles contain thinner microcracks which result in their reduced reactivity. If proven effective, annealing can serve as a new method for mitigation of ASR in recycled glass aggregates.

3. Materials and experiments

3.1. Annealing

To assess the effectiveness of annealing in removing the residual microcracks and potentially reducing the reactivity of glass particles, nine mortar mixtures were prepared with 100% glass sand and tested according to ASTM C1260. Details of the mixture proportions and the annealing procedure are provided in Table 1. All mortars were prepared with $w/c = 0.47$, using a type I Portland cement with oxide composition provided in Table 2. Mortars H1 to H7 contained 53% volume fraction mixed-color glass sand with gradation in the range #4–#100 sieves (4.75 mm to 150 μm) according to ASTM C1260 requirements. The last two mortars (SH1 and SH2) contained amber color glass sand in the narrow size range #8–#16 sieves (1.18–2.36 mm; i.e., the pessimum size based on Fig. 1). To ensure proper workability, a reduction in the sand volume fraction from 53% to 34% was necessary in these mortars. Mortar H1 served as the control mixture with non-annealed glass sand. In other mortars (i.e., H2–H7), only the more reactive size fraction of glass (between #4 and #30 sieves [22]) was annealed while the smaller sizes were used without heat treatment.

Annealing was performed inside a programmable furnace. As illustrated in Fig. 3, glass was heated at a rate 6.7 °C/min to 500 °C, followed by a rate 15 °C/min, up to a pre-defined peak temperature (Table 1), held at the peak temperature between 1 and 40 min to allow healing of the microcracks, and then cooled at a slow rate of approximately 1.7 °C/min to prevent thermal cracking. The peak temperatures were selected in a range in which soda-lime glass starts to behave as a Newtonian fluid with viscosities lower than 10^{11} Pa s [26].

Mortars were batched and mixed according to ASTM C305. From each mixture, four mortar bars ($25 \times 25 \times 250$ mm) were cast with stainless steel gage studs embedded at the opposite 25×25 mm faces to facilitate length measurements (ASTM C490). After 24 h of curing in moist room, specimens were demolded, cured for an additional 24 h submerged in water at 80 °C, followed by submerging inside a 1 N NaOH solution at 80 °C to provide an accelerated ASR environment. Expansions were monitored by measuring the length of specimens over a 14 day test period, using a digital comparator with precision 0.0025 mm.

Table 1
Information on mortars made with glass sand annealed at different temperatures and durations.

Mix ID	Gradation (mesh size)	Sand vol. fraction	Peak temp. (°C)[a]	Hold time at peak temp. (min)[a]	Glass sand color
H1	#4–#100	0.53	–	–	Mixed
H2	#4–#100	0.53	560	40	Mixed
H3	#4–#100	0.53	600	40	Mixed
H4	#4–#100	0.53	650	40	Mixed
H5	#4–#100	0.53	680	40	Mixed
H6	#4–#100	0.53	650	1	Mixed
H7	#4–#100	0.53	650	20	Mixed
SH1	#8–#16	0.34	700	40	Amber
SH2	#8–#16	0.34	650	40	Amber

[a] Peak temperature and the hold time are defined in Fig. 3.

3.2. Scanning electron microscopy and image analysis

In parallel with expansion measurements, mortars SH1 and SH2 were also analyzed using SEM after 14 and 26 days of NaOH exposure to study the microstructure of mortars containing annealed glass. Cross sections were cut from representative mortar bars with diamond blade saw to approximately 1 cm thickness and the sections were vacuum dried for 2 days inside a desiccator. After drying, the samples were vacuum impregnated using a low viscosity epoxy resin. Once the epoxy had set, the top 1–2 mm of each sample was trimmed using a low-speed precision saw. The newly exposed surface was ground and polished with successively finer abrasive grits starting at 15 μm and finishing with 1 μm diamond powder. In order to prevent the leaching of ASR gel from samples, all polishing and grinding operations were performed using polishing oil instead of water. Finally, the polished samples were carbon coated prior to SEM analysis. A JEOL JSM-5900 LV Environmental SEM instrument was used to allow image acquisition. Images were taken in a backscattered mode using 15 kV voltage and 1 nA current.

SEM imaging was also performed on amber glass particles of three different size fractions to evaluate the extent and size of the residual microcracks induced by bottle crushing. The size ranges were 1.18–2.36 mm (#8–#16 mesh), 0.3–0.6 mm (#30–#50 mesh), and 0.075–0.15 mm (#100–#200 mesh). Representative particles from each size fraction were sieved out from crushed glass, washed, dried, and vacuum impregnated using an epoxy resin. Then a flat surface of epoxy-impregnated particles was obtained by polishing a trimmed surface using abrasive grits as described above.

The degree of glass microcracking was quantified by analysis of the backscattered electron (BSE) images obtained from a minimum of 10 representative particles from each of the three size fractions. For any observed crack in each glass particle, high magnification (up to ×10,000) images generated appropriate resolution to measure the crack width with precision 0.1 μm. Starting from one corner of a glass particle and going through the entire surface, wherever a crack was found, its magnified micrograph was captured. Using the AutoCAD software for image analysis, the crack widths were measured at 4–8 μm intervals along the length of each crack (Fig. 4). Therefore, in all glass particles examined, a digital record of all crack widths and lengths was generated. Cracks narrower than 1 μm were subsequently omitted from the analysis as these cracks were abundant and sometimes difficult to distinguish from scratches on particles surface (note that specimens were polished to 1 μm grit). After collection of the crack geometry data, the identified cracks were divided into two groups: cracks wider than 2.5 μm, and cracks narrower than 2.5 μm. The reason for choosing the 2.5 μm threshold is discussed in the results section.

4. Results

4.1. Effectiveness of annealing in mitigating ASR

ASR expansion measurements of mortars H1–H5 are provided in Fig. 5. These mortars were prepared with glass sand annealed

Table 2
Oxide composition (mass%) of the cement and glass (measured using XRF).

	CaO	SiO_2	Al_2O_3	Fe_2O_3	Na_2O	K_2O	MgO	TiO_2	SO_3	LOI
Portland cement	63.9	17.3	4.81	2.00	0.55	1.91	2.85	N/D	4.9	1.73
Glass (mix color)	10.9	71.4	1.74	0.93	13.0	0.73	0.80	0.09	N/D	0.35
Glass (amber)	12.4	74.4	1.28	0.18	10.3	0.35	0.50	N/D	N/D	0.64

N/D is not detected.

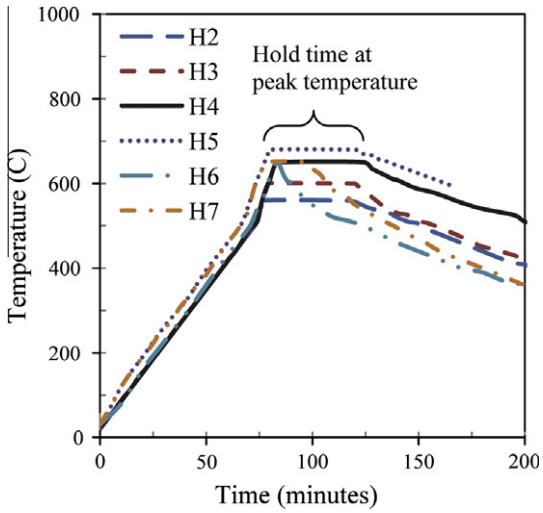

Fig. 3. Annealing procedure for crushed glass particles.

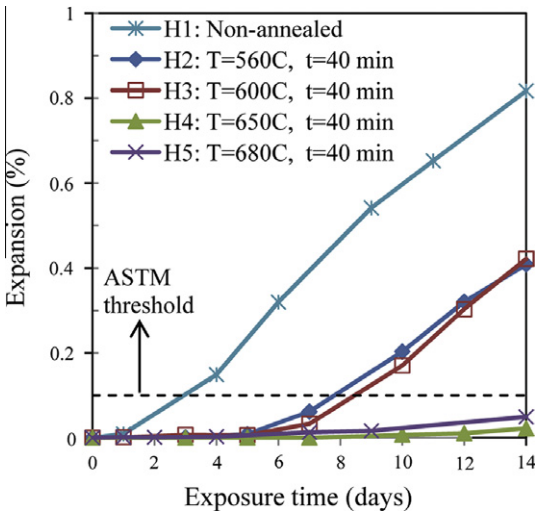

Fig. 5. ASR expansion of mortars made with glass sand annealed at different temperatures.

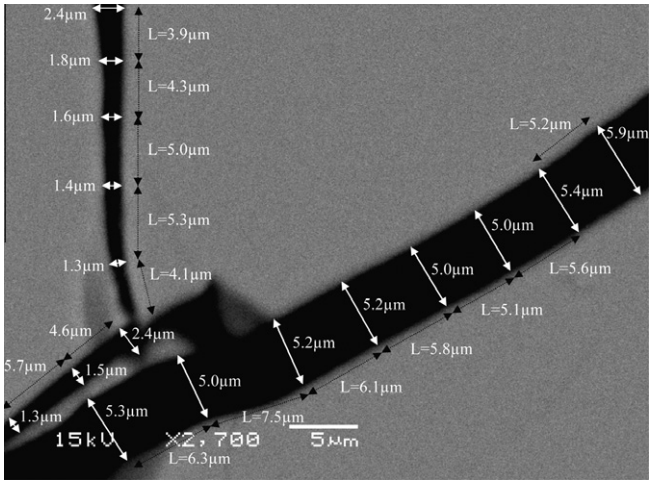

Fig. 4. Illustration of the image analysis procedure on residual cracks of a glass particle (glass size: 1.18–2.36 mm).

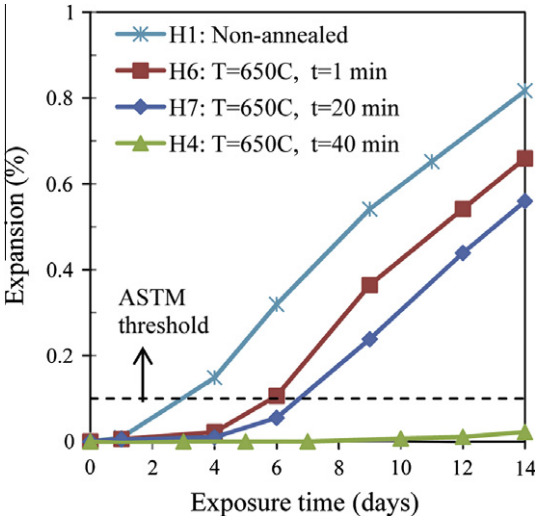

Fig. 6. ASR expansion of mortars containing glass sand with various annealing times.

at different temperatures (560–680 °C) with a hold time of 40 min. As expected, the control mortar H1, made with non-annealed glass, expands rapidly and significantly as a consequence of ASR and exceeds the ASTM C1260 threshold of 0.1% expansion at 14 days by more than eight times. The mortars containing glass sand annealed at 560 °C and 600 °C (i.e., H2 and H3) show comparable expansion trends with maximum 14 day expansions reduced to half of the control mixture. While annealing at these lower temperatures have been helpful, the expansions still exceed the ASTM threshold. Mortars H4 and H5, which contain glass annealed at 650 °C and 680 °C, demonstrate significantly reduced expansions which meet the ASTM criteria. In addition to the effect of annealing temperature, the effect of hold time at peak temperature on the reactivity of glass was examined using mortars H4, H6, and H7. Since crack healing is essentially a fluid flow process, and considering the high viscosity of glass, sufficient anneal time is needed to ensure that cracks are properly healed. The results, presented in Fig. 6, show that for glass annealed at 650 °C, a hold-time of at least 40 min is required to properly mitigate ASR expansions below the ASTM C1260 threshold of 0.1%.

Additional tests were performed on mortars SH1 and SH2 which were prepared using annealed mono-size amber color glass. Fig. 7 shows the ASTM C1260 expansion measurements. Both mortars show negligible expansions during a 14 day test period. It should be noted that these mortars contained a lower volume fraction of total sand (34%) comparing with the ASTM C1260 prescription (calculated as 53% based on the specific gravity of glass). However, if one considers only the volume fraction of reactive glass sizes (i.e., >#30 sieve [22]), ASTM prescription is equivalent to 32% sand which is comparable with mortars SH1 and SH2. In any case, the threshold expansion of 0.1% should not be directly applied to the results in Fig. 7. For mortar SH1, the test was continued until 26 days. Only after 19 days, expansions started to grow. This may suggest that very thin cracks may still exist inside glass even after annealing; due to incomplete healing, thermal cracking during the post-annealing cooling period, or cracking during handling and mixing in mortar. These thin cracks could eventually undergo ASR after prolonged exposure to the harsh NaOH environment. Would properly annealed recycled glass sand be sufficiently durable against ASR? The results presented in Fig. 5 suggest that it passes ASTM C1260 test; however, longer term tests such as ASTM C1293 is needed to confirm these results.

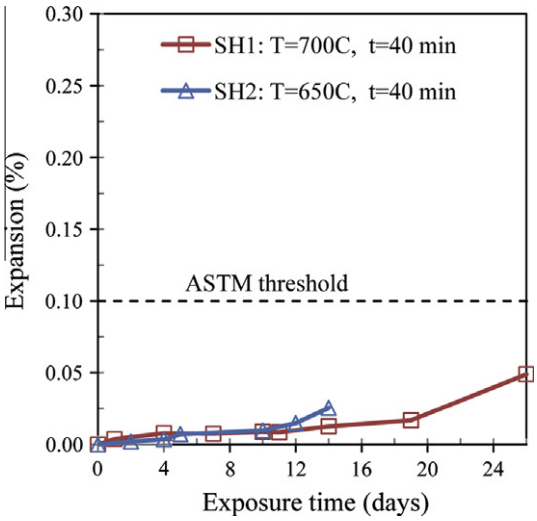

Fig. 7. ASR expansion of mortars with annealed, mono-size, amber glass sand.

SEM imaging of annealed glass particles shows healing of the residual microcracks. Fig. 8a shows glass sand annealed at 700 °C for 40 min. The particles were impregnated with epoxy after annealing. Comparing this image with Fig. 2b, which shows non-annealed glass, it is evident that annealing has effectively removed the residual microcracks. It is also observed in Fig. 8a that some corners of adjacent glass particles have fused together during the annealing process and have created weak bounds, which necessitated using some force to separate the particles after the batch of glass had been cooled. Care must be taken in this process to prevent creation of secondary microcracks in the particles, which may later act as ASR initiation sites. A representative SEM micrograph of a cross section of mortar SH1 after 26 days of NaOH exposure is shown in Fig. 8b. No ASR deterioration is observed within or at the perimeter of glass particles, which shows the effectiveness of annealing in removal of residual cracks and mitigation of ASR.

4.2. SEM image analysis to quantitate residual cracks in crushed glass

Preliminary image analysis of crushed glass particles showed that the larger size fraction (i.e., glass retained between #8 and #16 sieves) contains wider microcracks in comparison with finer particles (i.e., retained between #30–#50 mesh and #100–#200 mesh). In parallel, examination of SEM images from mortars with non-annealed glass (H1 in this work as well as several mortars from [14]) revealed that there are thin cracks within glass particles that have not undergone ASR after 14 days of NaOH exposure. Fig. 9 shows an example in which a glass particle in the size range #8–#16 mesh contains ASR affected cracks as well as thin unaffected microcracks. Since the initiation and propagation of ASR depends on diffusion of hydroxyl and alkali ions as well as permeation of water inside the microcracks, and since the transport properties of cracks are dependent on crack size (e.g., permeability is a function of crack width square [27,28]), it is anticipated that smaller cracks undergo ASR at a slower rate. For very thin cracks, the rate may be significantly slower to the point that during the ASTM C1260 test, ASR gel does not form within these cracks in quantities that are detectable by SEM. Careful examination of mortars showed that a critical crack width of approximately 2.5 μm exists such that smaller cracks remain free of ASR gel at the conclusion of ASTM C1260 test.

As described in Section 3.2, through SEM image analysis of crushed glass particles, a digital record of all crack widths larger than 1 μm was generated. Further, the identified cracks were divided into two groups: those that are larger than the critical crack width of 2.5 μm, and those that are smaller. For each size fraction of glass particles studied (i.e., #8–#16, #30–#50, and #100–#200), the percentage of reactive microcracks (>2.5 μm) was calculated by

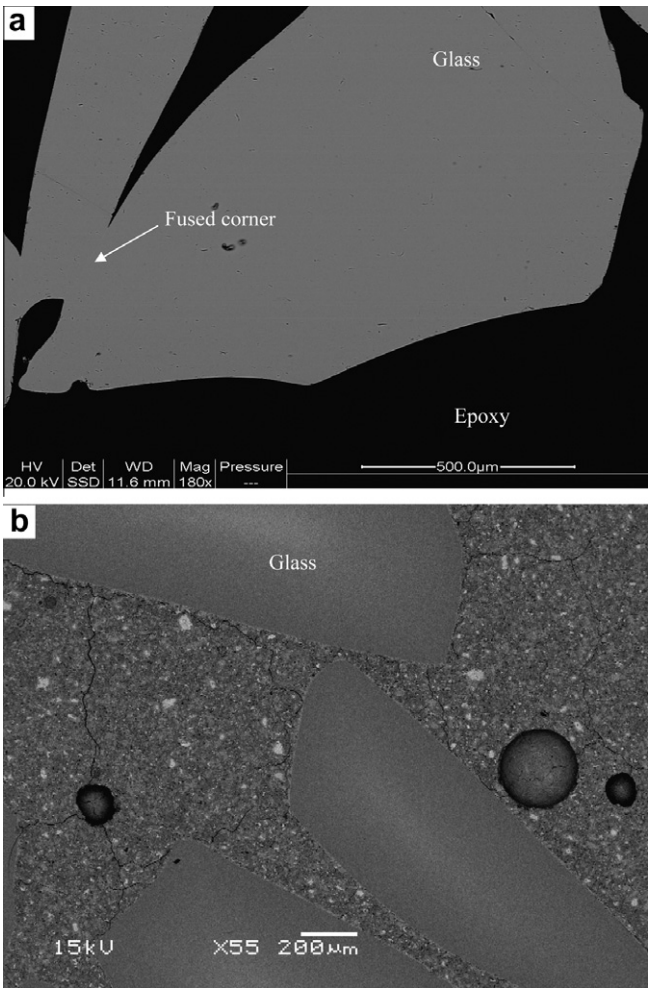

Fig. 8. (a) BSE image of glass sand annealed at 700 °C for 40 min (SH1) and (b) Image of mortar SH1 made with such sand after 26 days exposure to ASTM C1260 test.

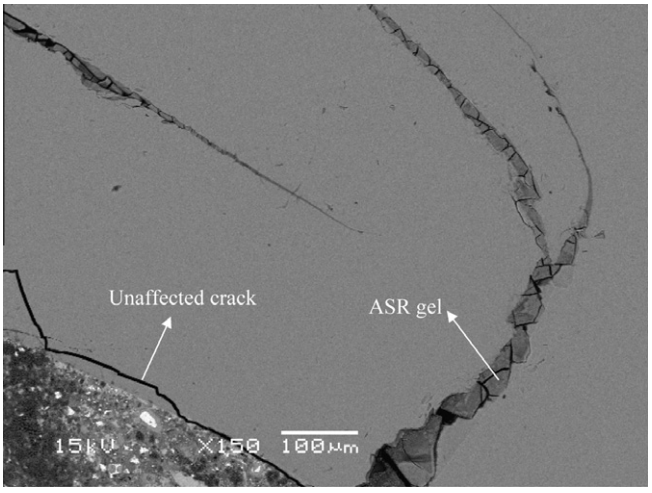

Fig. 9. Affected and unaffected cracks in mortars with 1.18–2.36 mm glass particles after exposure to ASTM C1260 condition for 14 days.

Table 3
Results of image analysis of glass particles showing parentage of cracks smaller and larger than the critical width (2.5 μm).

Glass particle size	1.18–2.36 mm (#8–#16) (%)	0.3–0.6 mm (#30–#50) (%)	0.075–0.15 mm (#100–#200) (%)
1 μm < Width < 2.5 μm	60.4	96.9	100
Width > 2.5 μm	39.6	3.1	0

dividing the length of these cracks by the total length of detected cracks larger than 1 μm. The results are presented in Table 3 which shows that for large glass particles (#8–#16 mesh), nearly 40% of all recorded cracks are wider than 2.5 μm, while finer particles include only 3% and 0% of reactive cracks for particles in the size range #30–#50, and #100–#200 mesh, respectively. This observation can offer a new explanation for the origin of the unusual size effect of the alkali-silica reactivity of glass particles. Larger particles are more reactive since they contain a higher percentage of residual microcracks larger than 2.5 μm, which are believed to be responsible for occurrence of ASR in mortars containing recycled glass sand.

5. Discussion

The results obtained in this paper confirm and strengthen the hypothesis that residual cracks in crushed glass particles serve as reaction sites for formation of ASR gel. As the gel absorbs water and swells, stress concentration at crack tips and sharp corners can result in propagation of new cracks which can themselves undergo ASR and induce a progressive damage. It was discussed that thin microcracks react at a slower rate and cracks below a critical width of 2.5 μm can remain intact after 14 days of NaOH exposure in ASTM C1260 test. Most importantly, it was observed that by healing the residual microcracks through proper annealing of crushed glass, the ASR expansions are significantly mitigated and mortars with 100% glass sand can easily pass ASTM C1260 test with 14 day expansions below 0.05%.

The authors acknowledge that ASR mitigation though annealing can be energy intensive and a cost-benefit analysis is required to further evaluate the merits of this technique. In this work, annealing was primarily adopted to evaluate the hypothesis that the residual microcracks are responsible for ASR in recycled glass. Nevertheless, annealing can be a prominent candidate when access to other ASR mitigation techniques (e.g., use of fly ash or lithium-based admixtures) is economically or legally unfavorable. For example, in the state of Hawaii, there is a limit of 5% (based on weight of dry constituents) on the use of fly ash in concrete due to potential health concerns related to presence of heavy metals in the ash. This low level of fly ash (equivalent to approximately 15% weight of cement) is insufficient for controlling ASR. As such annealing can be considered as an alternative or a complementary technique.

Moreover, optimizing the annealing process can result in significant energy savings by finding the most efficient annealing temperature, hold time, and heating rates. The time-temperature relationship of the annealing process can be studied as a viscous flow problem in which the time it takes to remove a known flaw size (i.e., strain) by flowing of a liquid of known temperature-dependent viscosity is calculated. The driving force for healing is the surface energy of glass which can generate strong capillary forces at a curved glass–air interface (e.g., at the tip of a microcrack). Since soda-lime glass behaves as a Newtonian fluid above its glass transition temperature (520–550 °C [26]), as a first approximation, the healing time can be directly related to the viscosity of glass according to Newton's law:

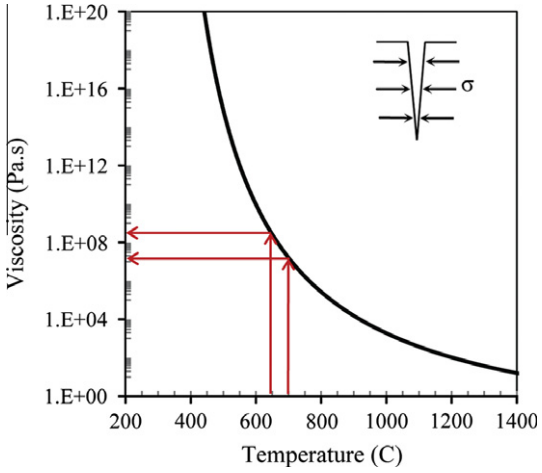

Fig. 10. Temperature dependency of viscosity for soda-lime glass (data from [26]).

$$t_{heal} = \frac{\varepsilon}{\sigma}\lambda(T) \quad (1)$$

where ε (m/m) is the strain (related to crack width), σ (Pa) is the capillary-induced stress, and λ (Pa s) is the viscosity of glass at temperature T. Fig. 10 shows the viscosity-temperature relationship for soda-lime glass. At 650 °C, the viscosity is approximately $\lambda = 26 \times 10^7$ Pa s. Based on the experiments discussed earlier (e.g., Fig. 6), the required healing time at this temperature is 40 min. As an alternative, if the temperature is raised to 700 °C, viscosity is reduced to approximately $\lambda = 16 \times 10^6$ Pa s, resulting in a healing time of only $40 \times 16/260 = 2.5$ min. This is a preliminary estimation and the exact kinetics of the healing process should be studied through rheological modeling and experimental verification. Nevertheless, this estimation shows that optimizing the annealing time-temperature relationship can considerably improve the productivity and energy efficiency of the annealing process.

Another remaining question that should be studied in future research is "Why glass–cement paste interface does not undergo ASR?" The authors' preliminary opinion is that formation of a protective calcium-silicate-hydrate (C-S-H) gel which was observed in [14,22] could significantly reduce the dissolution rate of glass as suggested by Tarnopol and Junge [29], and Iler [30]. In addition, presence of portlandite at the interface favors formation of C-S-H instead of ASR gel [31]. Another explanation could be the availability of chemically reactive sites on the surface of interior microcracks which have not undergone weathering in comparison to the outer surface of glass particle. Also, the dissolved silica and sodium in the interior cracks are confined to a limited space which favors polymerization of silica in the form of ASR gel. These conditions can be very different at the glass–paste interface. This question is the subject of our ongoing research.

6. Conclusions

Based on the findings of this research, the following conclusions can be drawn:

- The residual cracks in the interior of recycled glass particles are responsible for the alkali-silica reactivity of glass. These cracks are formed during bottle crushing, and can further propagate by ASR.
- Annealing which exposes glass cullet to elevated temperatures can effectively heal cracks, and mitigate alkali-silica reaction. It was found that the reactive size fraction of glass cullet (between #4 and #30 sieves), when annealed at 650 °C for

40 min, becomes free of residual microcracks (based on SEM imaging), and mortars prepared with such glass sand pass ASTM C1260 test.

- The reactivity of residual microcracks depends on their size. Cracks thinner than a critical width of approximately 2.5 μm were found to remain intact after 14 days of ASTM C1260 test. Further, image analysis of SEM micrographs of glass cullet in different size fractions showed that larger glass particles include a significantly higher percentage of reactive microcracks (>2.5 μm) which could explain why larger particles are alkali-silica reactive while smaller glass particles are innocuous.

Acknowledgements

The authors gratefully acknowledge the financial support provided by Hawaii Department of Transportation (HDOT) and the Federal Highway Administration (FHWA). Any opinions, findings and conclusions or recommendations expressed in this material are those of the authors and do not necessarily reflect the views of HDOT or FHWA. The authors are very thankful to Dr. Carlo Pantano for his invaluable suggestions, and to Ms. JoAnn Sinton for her help and advice during SEM sample preparations.

References

[1] Reindl J. Reuse/recycling of glass cullet for non-container uses. <http://www.glassonline.com/infoserv/Glass_recycle_reuse/Glass_reuse_recycling_doc1.pdf> [accessed 30.11.10].
[2] US Environmental Protection Agency (EPA), Washington, DC. Municipal solid waste generation, recycling, and disposal in the United States: facts and figures for 2008, 2009. <http://www.epa.gov/osw/nonhaz/municipal/pubs/msw2008rpt.pdf> [accessed 30.11.10].
[3] Byars EA, Morales B, Zhu HY. Conglasscrete I. University of Sheffield. The Waste & Resources Action Programme; 2004.
[4] Shayan A, Xu AM. Value-added utilisation of waste glass in concrete. Cem Concr Res 2004;34(1):81–9.
[5] Jin W, Meyer C, Baxter S. Glascrete – concrete with glass aggregate. ACI Mater J 2000;97(2):208–13.
[6] Rajabipour F, Fischer G, Sigurdardottir P, Goodnight S, Leake A, Smith E. Recycling and utilizing waste glass as concrete aggregate. In: Transportation Research Board (TRB) 88th annual meeting, Washington, DC; 2009 [Paper #09-2195].
[7] Taha B, Nounu G. Utilizing waste recycled glass as sand/cement replacement in concrete. ASCE J Mater Civ Eng 2009;21(12):709–21.
[8] Polley C, Cramer SM, Da La Cruz RV. Potential for using waste glass in Portland cement concrete. ASCE J Mater Civ Eng 1998;10(4):210–9.
[9] Schmidt A, Saia WHF. Alkali aggregate reaction tests on glass used for exposed aggregate wall panel work. ACI Mater J 1963;60:1235–6.
[10] Johnson CD. Waste glass as coarse aggregate for concrete. J Test Eval 1974;2(5):344–50.
[11] Figg JW. Reaction between cement and artificial glass in concrete. In: 5th International conference on concrete alkali aggregate reactions (ICAAR), Cape Town, South Africa; 1981. p. 252–7.
[12] Mukherjee PK, Bickley JA. Performance of glass as concrete aggregates. In: 7th International conference on concrete alkali aggregate reactions (ICAAR), Ottawa, Canada; 1986. p. 36–42.
[13] Zhu HY, Byars EA. Alkali-silica reaction of recycled glass in concrete. In: 12th International conference on concrete alkali aggregate reactions (ICAAR), Beijing, China; 2004. p. 811–20.
[14] Maraghechi H. Utilization of recycled glass as sand or cement replacement in concrete materials. MSc thesis. Honolulu, University of Hawai'i-Manoa, 2010.
[15] Stanton TE. Expansion of concrete through reaction between cement and aggregate. In: Proceedings American Society of Civil Engineers, vol. 66; 1940. p. 1781–811.
[16] Vivian HE. The effect on mortar expansion of particle size of the reactive component in aggregate. Aust J Appl Sci 1951;2:488–92.
[17] Diamond S, Thaulow NA. A study of expansion due to alkali-silica reaction as conditioned by grain size of the reactive aggregate. Cem Concr Res 1974;4(4):591–607.
[18] Hobbs DW, Gutteridge WA. Particle size of aggregate and its influence upon the expansion caused by the alkali-silica reaction. Mag Concr Res 1979;31(109):235–42.
[19] Bažant ZP, Steffens A. Mathematical model for kinetics of alkali-silica reaction in concrete. Cem Concr Res 2000;30(3):419–28.
[20] Bažant ZP, Zi G, Meyer C. Fracture Mechanics of ASR in concretes with waste glass particles of different sizes. J Eng Mech 2000;126(3):226–32.
[21] Suwito A, Jin W, Xi Y, Meyer C. A mathematical model for the pessimum size effect of ASR in concrete. Concr Sci Eng 2002;4(13):23–34.
[22] Rajabipour F, Maraghechi H, Fischer G. Investigating the alkali silica reaction of recycled glass aggregates in concrete materials. ASCE J Mater Civ Eng 2010;22(12):1201–8.
[23] Dyer TD, Dhir RK. Chemical reactions of glass cullet used as cement component. ASCE J Mater Civ Eng 2001;13(6):412–7.
[24] Schwarz N, Neithalath N. Influence of fine glass powder on cement hydration: Comparison to fly ash and modeling the degree of hydration. Cem Concr Res 2008;38(4):429–36.
[25] Shao Y, Lefort T, Moras S, Rodriguez D. Studies on concrete containing ground waste glass. Cem Concr Res 2000;30(1):91–100.
[26] National Institute of standards and Technology (NIST): Standard Reference Material 710A: soda-lime–silica glass, Gaithersburg, MD 20899, March, 1991.
[27] Dietrich P, Helmig R, Sauter M, Hotzl H, Kongeter J, Teutsch G. Flow and transport in fractured porous media. The Netherlands: Springer; 2005.
[28] Akhavan A, Shafaatian S, Rajabipour F. Quantifying the effect of crack width, tortuosity, and roughness on water permeability of cracked mortars. Cem Concr Res, submitted for publication.
[29] Tarnopol MS, Junge AE. Resistance of plate glass to alkaline solutions. J Am Ceram Soc 1946;29(2):36–9.
[30] Iler RK. Chemistry of silica – Solubility, polymerization, colloid and surface properties and biochemistry. New York: John Wiley & Sons; 1979.
[31] Hou X, Struble LJ, Kirkpatrick RJ. Formation of ASR gel and the roles of C–S–H and portlandite. Cem Concr Res 2004;34(9):1683–96.